**A**

| Position | Codon | Possible residues |
|----------|-------|-------------------|
| V39 | NDT | CDFGHILNRSVY |
| N41 | RWT | NIVD |
| Y43 | HWT | FYLHIN |
| M45 | VWG | EKLMQV |
| S48 | VNT | ADGHILNPRSTV |
| N49 | NDT | CDFGHILNRSVY |
| Q50 | VWW | HQNKDELIV |
| T51 | VYT | AILPTV |
| D52 | NDT | CDFGHILNRSVY |
| K53 | VNA | AEGIKLPQTVR |
| A56 | NHT | ADFHILNPSTVY |
| Q63 | VNA | AEGIKLPQTVR |
| G65 | NDT | CDFGHILNRSVY |
| Q66 | CMA | QP |
| L97 | NWT | FILVYHND |
| S102 | NCT | STAP |
| L103 | NDT | CDFGHILNRSVY |
| A104 | NHT | ADFHILNPSTVY |
| P105 | SCT | AP |
| K106 | VNA | AEGIKLPQTVR |
| A107 | NYT | FILVSPTA |
| E111 | VRW | DEHKNQSGR |

**B**
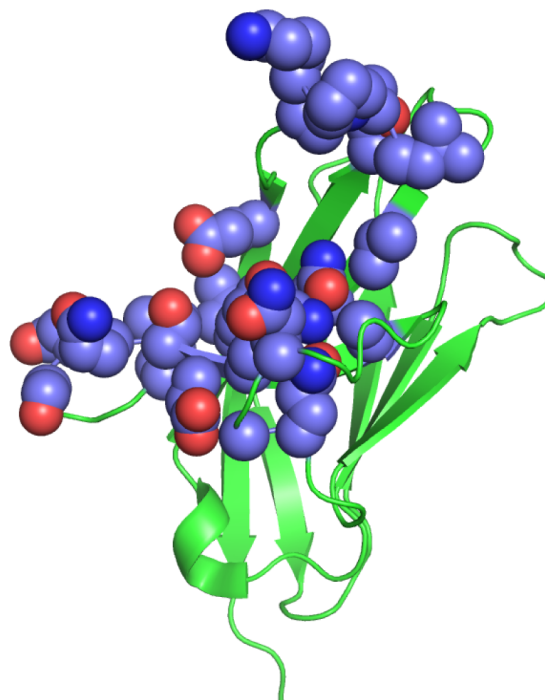


**Figure S1.** Design of the "First Generation" PD-1 library. (*A*) Table of randomized positions of hPD-1 are given in the table, with the corresponding degenerate codon and the potential amino acids possible at each site.  (*B*) Structural depiction of the "First Generation" library; hPD-1 is in green with randomized side chains indicated as blue space-filling spheres.

**A**

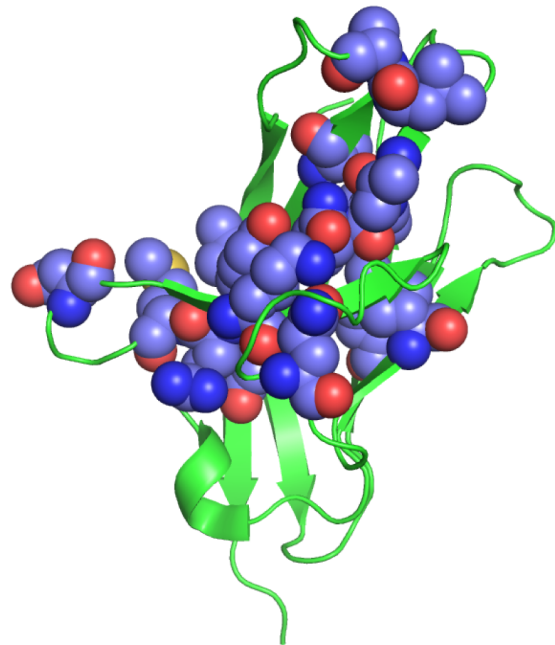| Position | Codon | Possible residues |
|----------|-------|-------------------|
| V39 | VRT | DGHNRS |
| L40 | NTT | FILV |
| N41 | NWT | FILVDHNY |
| Y43 | YWT | FHLY |
| R44 | YDT | FHLRYC |
| M45 | SAW | DEHQ |
| N49 | DRT | CDGNSY |
| K53 | AMA | KT |
| Q66 | CMA | QP |
| V72 | RYT | VAIT |
| M83 | NTS | FILVM |
| Y96 | YWT | FHLY |
| L97 | NTT | FILV |
| A100 | RYT | VAIT |
| L103 | YWT | FHLY |
| A107 | NTT | FILV |

**B**



**Figure S2.** Design of the "Second Generation" PD-1 library. (*A*) Table of randomized positions of hPD-1 are given in the table, with the corresponding degenerate codon and the potential amino acids possible at each site. (*B*) Structural depiction of the "Second Generation" library; hPD-1 is in green with randomized side chains indicated as blue space-filling spheres.
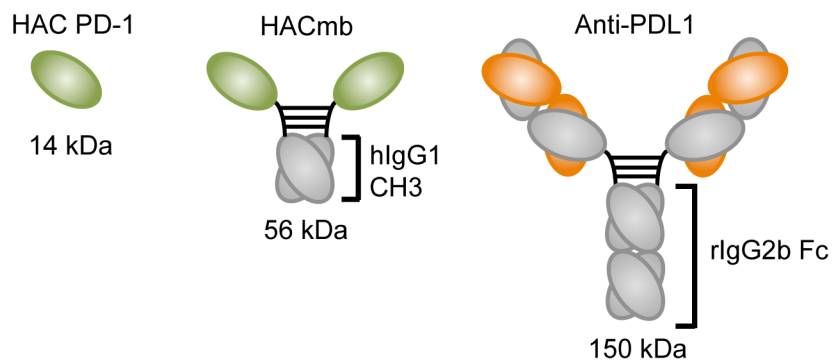
**Figure S3.** Schematic diagram of HAC "microbody" (HACmb) design in comparison to individual HAC PD-1 monomer and anti-PD-L1 antibody. HACmb is HAC-V fused to the CH3 domain of human IgG1 linked by a disulfide-containing hinge sequence.
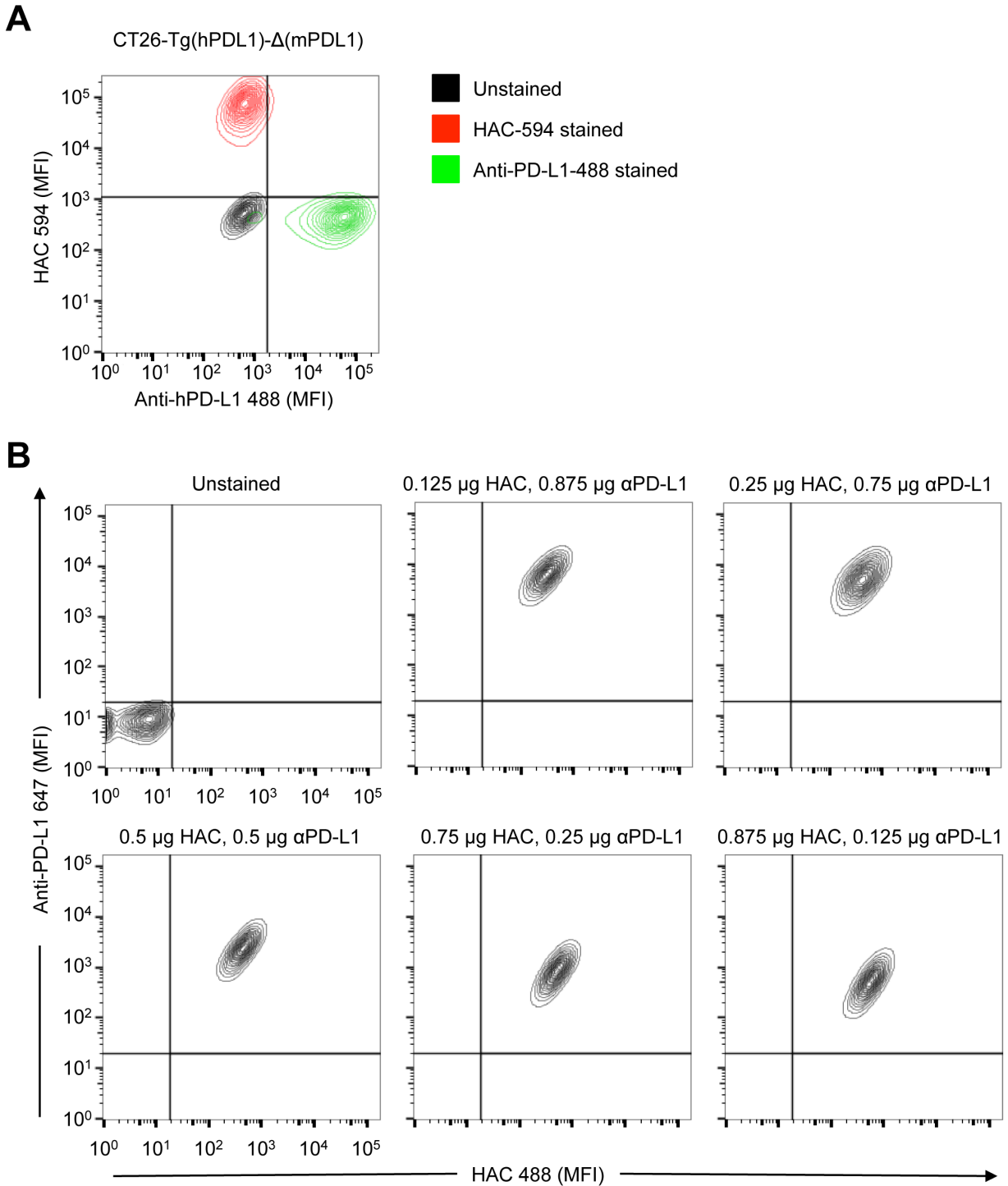
**Figure S4** *In vitro* staining of hPD-L1 expressing cells. (*A*) FACS plot of CT26-Tg(hPD-L1)-Δ(mPDL1) either unstained (black), stained with AlexaFluor594-labeled HAC monomer (red), or AlexaFluor488-labeled anti-PD-L1 antibody (clone 29E.2A3, Biolegend). (*B*) *In vitro* competitive staining of hPD-L1-expressing CT26 cells using a titrated range of HAC labeled with Alexa Fluor-488 and anti-human PD-L1 (clone 29E.2A3) labeled with APC. Antibody and HAC quantities are labeled below each plot.
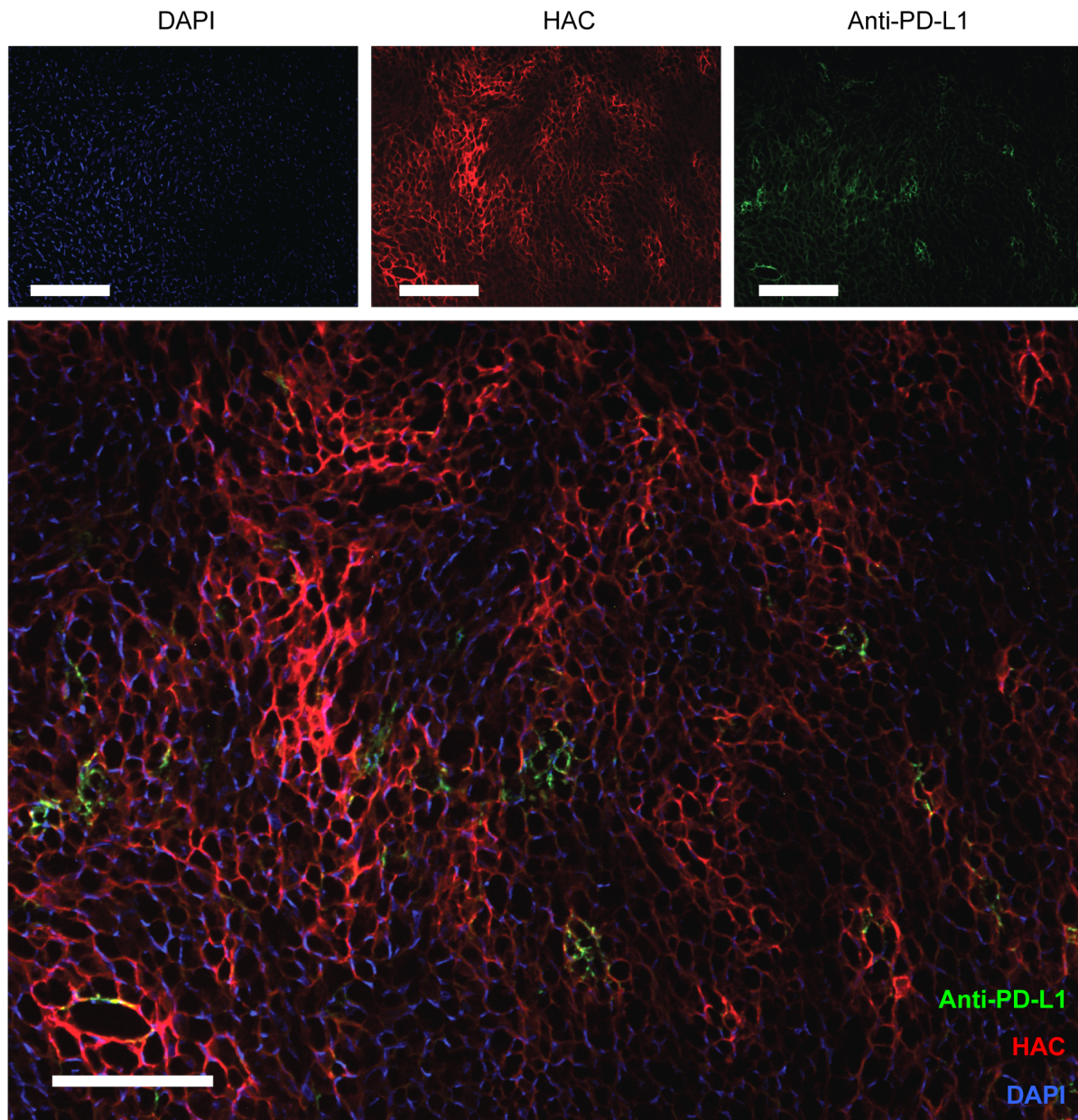
**Figure S5.** *In vivo* staining of hPD-L1-expressing tumors. Histological section taken from the same tumor as depicted in Figure 3A, but from the center of the tumor rather than at the periphery. Image is from tumors dissected four hours after intraperitoneal injection of anti-hPD-L1-Alexa Fluor488 (green) and HAC-Alexa Fluor 594 (red). Nuclei (blue) were labeled with DAPI. Scale bars represent 500µm.
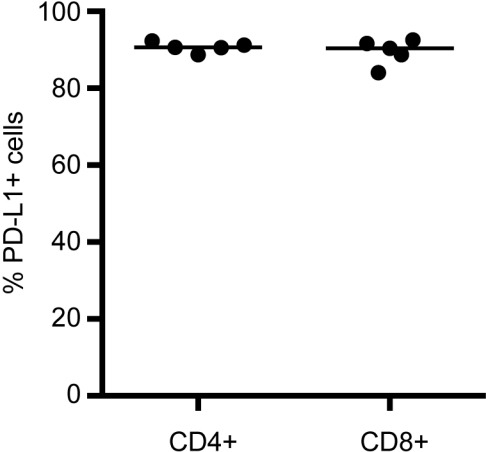
**Figure S6.** PD-L1 is expressed on the surface of circulating T cells in tumor-engrafted mice. Dot plot of % positive PD-L1 expression by CD4+ T cells (left) and CD8+ T cells (right), as measured by FACS analysis of lymphocytes from the peripheral blood of mice 14 days post-engraftment with CT26 tumors.
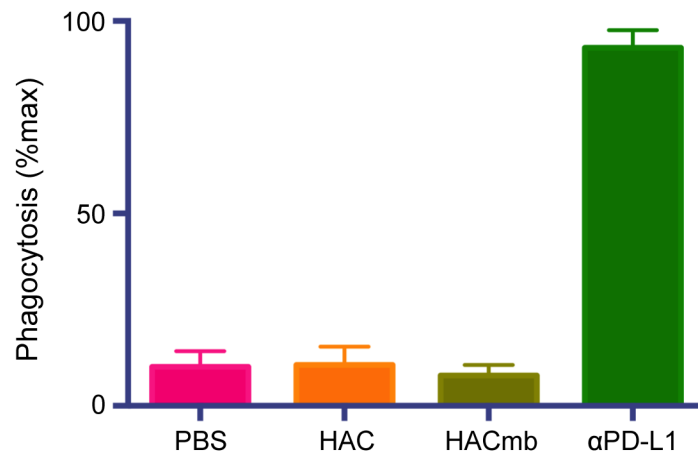
**Figure S7.** HACmb does not induce macrophage-mediated phagocytosis *in vitro*. FACS-based phagocytosis assay using *ex vivo* differentiated human macrophages and CFSE-labeled hPD-L1 expressing CT26 cells as target. Y axis represents the percent of CFSE+ macrophages after co-culture with CT26 target cells and either HAC monomer, HACmb, or anti-human PD-L1 (clone 29E.2A3).
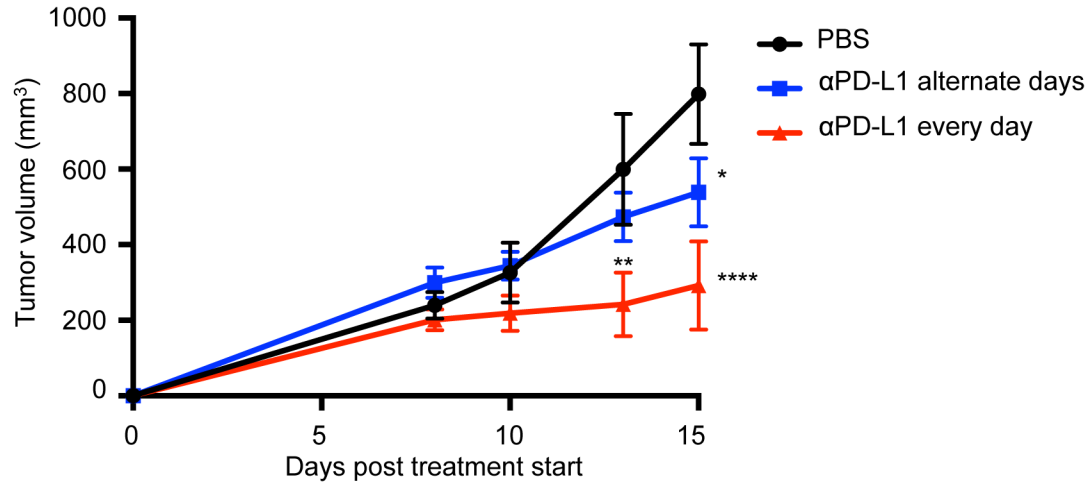
**Figure S8.** Dose-finding study of anti-mPD-L1 antibody 10F.9G2 in the CT26 syngeneic tumor model. Relative growth rates of engrafted tumors, calculated as tumor volume (mm$^3$) based on thrice-weekly caliper measurement of individual tumors over the course of the treatment period. Mice were engrafted subcutaneously with 5x10$^6$ CT26 cells, and treatment with either vehicle (PBS, black), thrice-weekly anti-mPD-L1 antibody (blue), or daily anti-mPD-L1 antibody (red) was begun the day after engraftment. Error bars represent s.e.m. *, p<0.05, **, p<0.01, ****, p<0.0001.
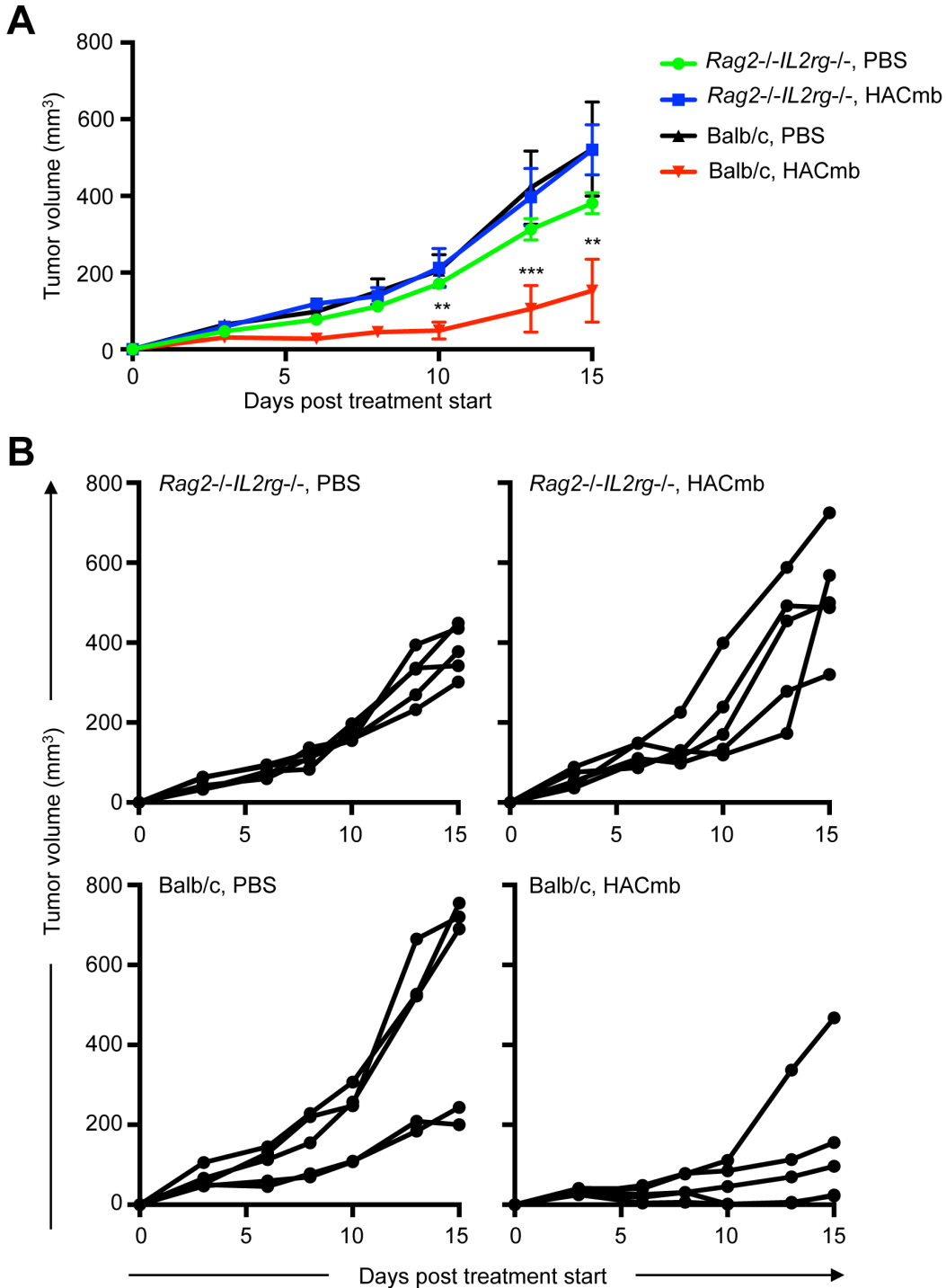
**Figure S9.** Anti-tumor activity of HACmb requires adaptive immunity. Relative growth rates of engrafted tumors, calculated as tumor volume (mm$^3$) based on thrice-weekly caliper measurement of individual tumors over the course of the treatment period. Either wild-type Balb/c mice or immunocompromised *Rag2-/-IL2Rg-/-* mice were engrafted subcutaneously with 1x10$^6$ CT26 cells, and treatment with either vehicle (PBS), or daily HACmb was initiated the day after engraftment. Error bars represent s.e.m. **, p<0.01, ***, p<0.001.
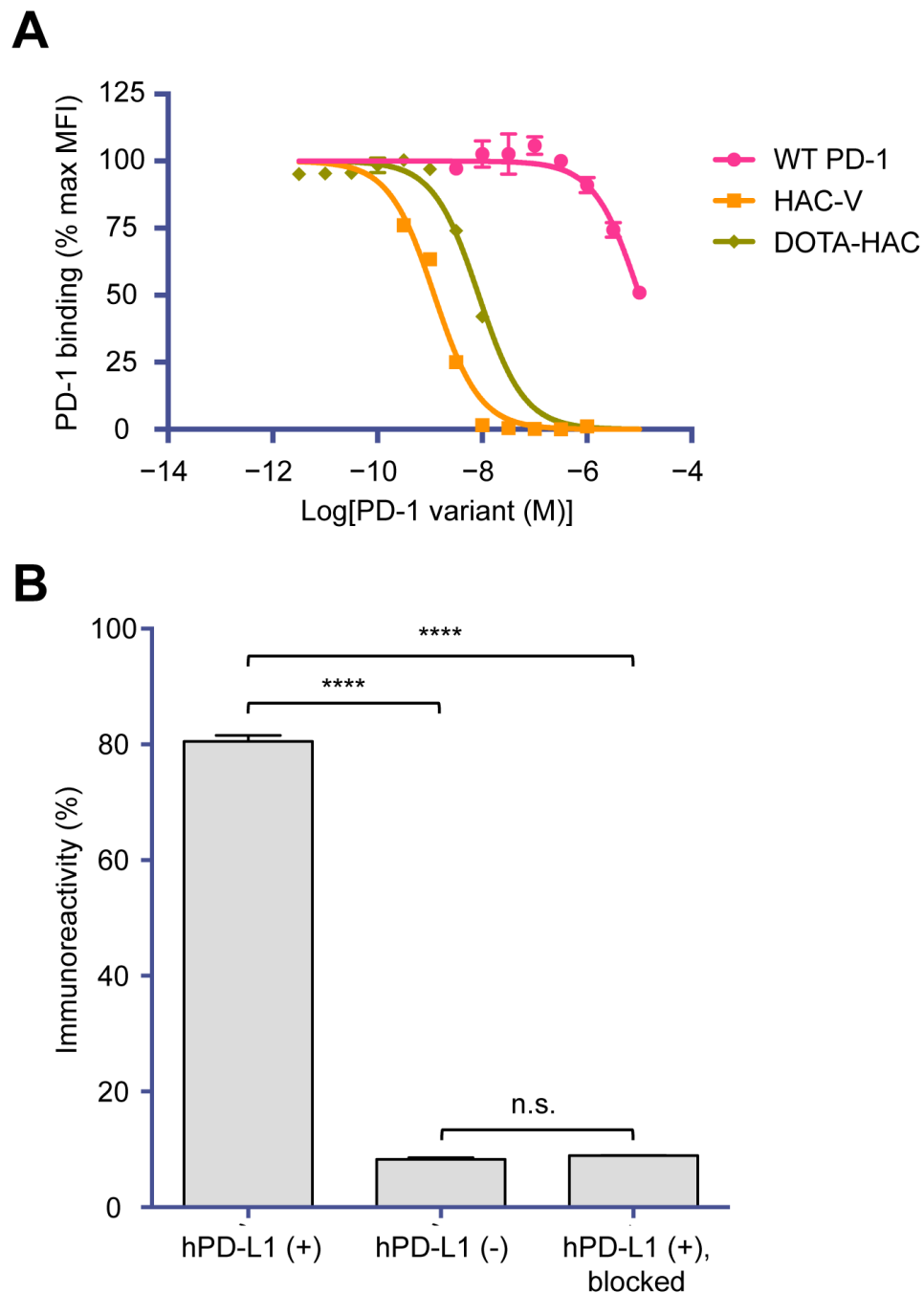
**Figure S10.** Validation of DOTA-HAC PET tracer. (*A*) Competition binding assays of wild-type hPD-1, HAC-V, or DOTA-HAC on human SK-MEL-28 cells. 100 nM hPD-1/streptavidin-Alexa Fluor 647 tetramer was used as the probe ligand. Error bars represent s.e.m. (*B*) Immunoreactivity of anti-hPD-L1 radiotracer. hPD-L1(+), hPD-L1(-) and hPD-L1(+) cells blocked with excess HAC-N91C prior to the addition of tracer were tested for binding specificity. 5 nM $^{64}$Cu-DOTA-HAC readily bound to hPD-L1(+) cells (80.5 % ± 1.9 %),  while control hPD-L1(-) cells only exhibited minimal immunoreactivity (8.3 % ± 0.5 %). Binding was blocked in hPD-L1(+) cells by the addition of HAC-N91C to 1 µM (8.9 % ± 0.1 %). n.s., not significant. ****, p<0.0001, Two-way ANOVA.
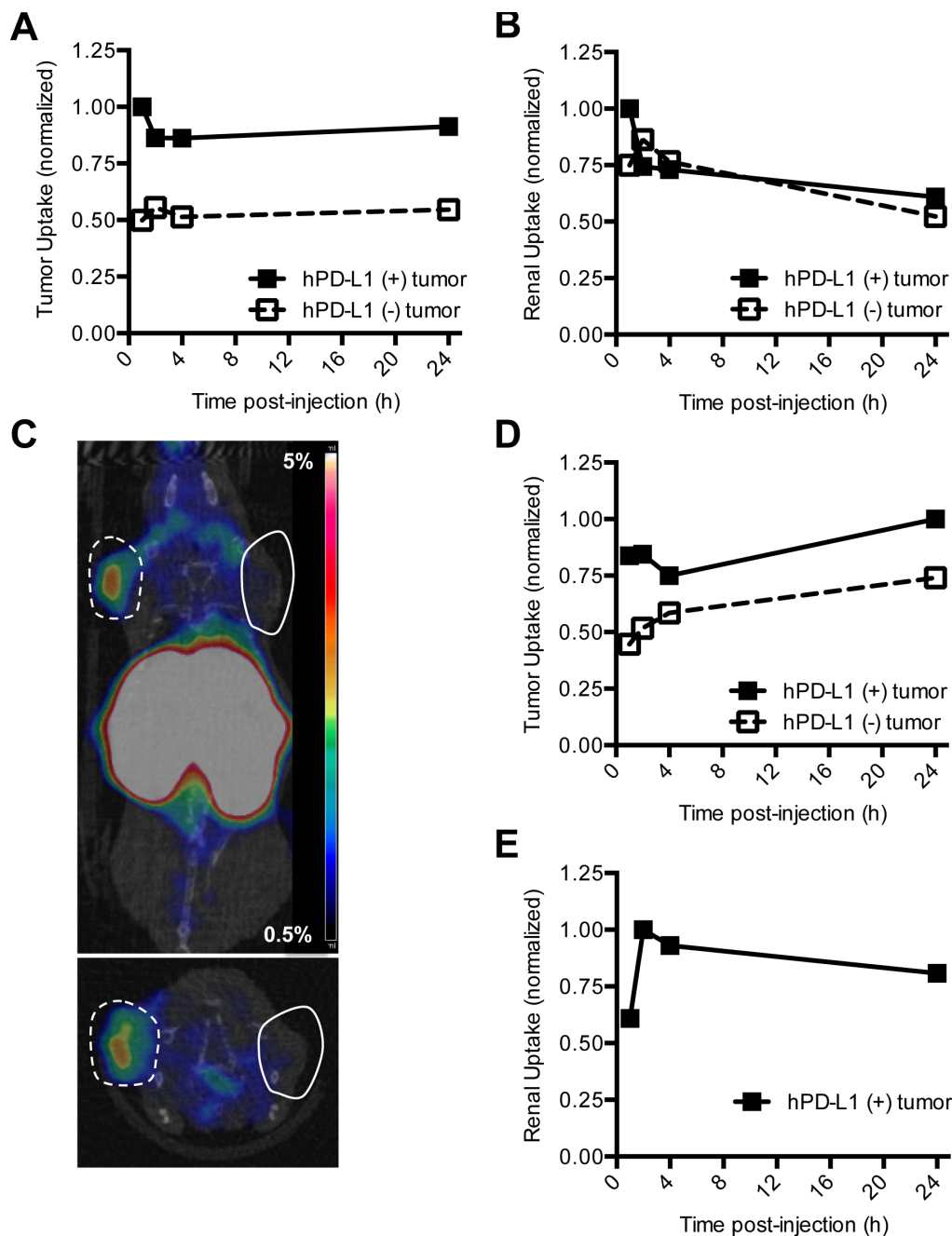
**Figure S11.** $^{64}$Cu-DOTA-HAC MicroPET imaging dynamics. (*A*) Tumor uptake computed by region of interest (ROI) analysis over 24 hours. (*B*) Renal uptake in hPD-L1 (+) and (-) tumor bearing mice assessed by ROI analysis. (*C*) PET-CT image 24 hours post-injection of $^{64}$Cu-DOTA-HAC (230µCi/25µg/200µl) in NSG mouse bearing dual subcutaneous hPD-L1(+) (dashed) and hPD-L1(-) (solid) CT26 tumors. (*D*) Tumor uptake computed by region of interest (ROI) in dual tumor bearing mice. (*E*) Renal clearance over 24 hours in dual tumor bearing mice. All uptake values normalized to maximum mean %ID/g. Normalized $(\mu_t) = \frac{\mu_t - \mu_{min}}{\mu_{max} - \mu_{min}}$, where $\mu_t$ is the average %ID/g for n mice at a given time point, $\mu_{max}$ is the maximum average %ID/g for all time points, and $\mu_{min}$ is equal to zero.

**A**



**B**

| Tumor : Normal Tissue Ratios | | |
|---|---|---|
| **Organ** | **1hr** | **24hrs** |
| Blood | 6.41 ± 1.26 | 2.38 ± 0.44 |
| Heart | 1.03 ± 0.05 | 2.81 ± 1.17 |
| Lungs | 4.11 ± 1.20 | 2.88 ± 0.66 |
| Liver | 0.09 ± 0.01 | 0.20 ± 0.01 |
| Spleen | 0.65 ± 0.33 | 0.89 ± 0.52 |
| Pancreas | 1.49 ± 0.47 | 1.93 ± 0.84 |
| Stomach | 2.16 ± 1.09 | 1.53 ± 0.18 |
| Sm Intestine | 1.19 ± 0.59 | 1.77 ± 0.54 |
| Lg Intestine | 2.36 ± 1.46 | 1.73 ± 0.29 |
| Kidney | 0.02 ± 0.001 | 0.16 ± 0.08 |
| Muscle | 6.77 ± 2.01 | 6.40 ± 1.34 |
| Bone | 1.01 ± 0.44 | 1.77 ± 0.28 |
| Bonemarrow | 31.69 ± 17.26 | 61.89 ± 34.99 |
| Skin | 3.10 ± 1.61 | 7.04 ± 0.12 |
| Brain | 31.13 ± 7.20 | 43.01 ± 5.57 |
| Tumor (-) | 4.23 ± 3.96 | 1.82 ± 0.33 |
| Tail | 1.17 ± 0.25 | 2.08 ± 0.39 |

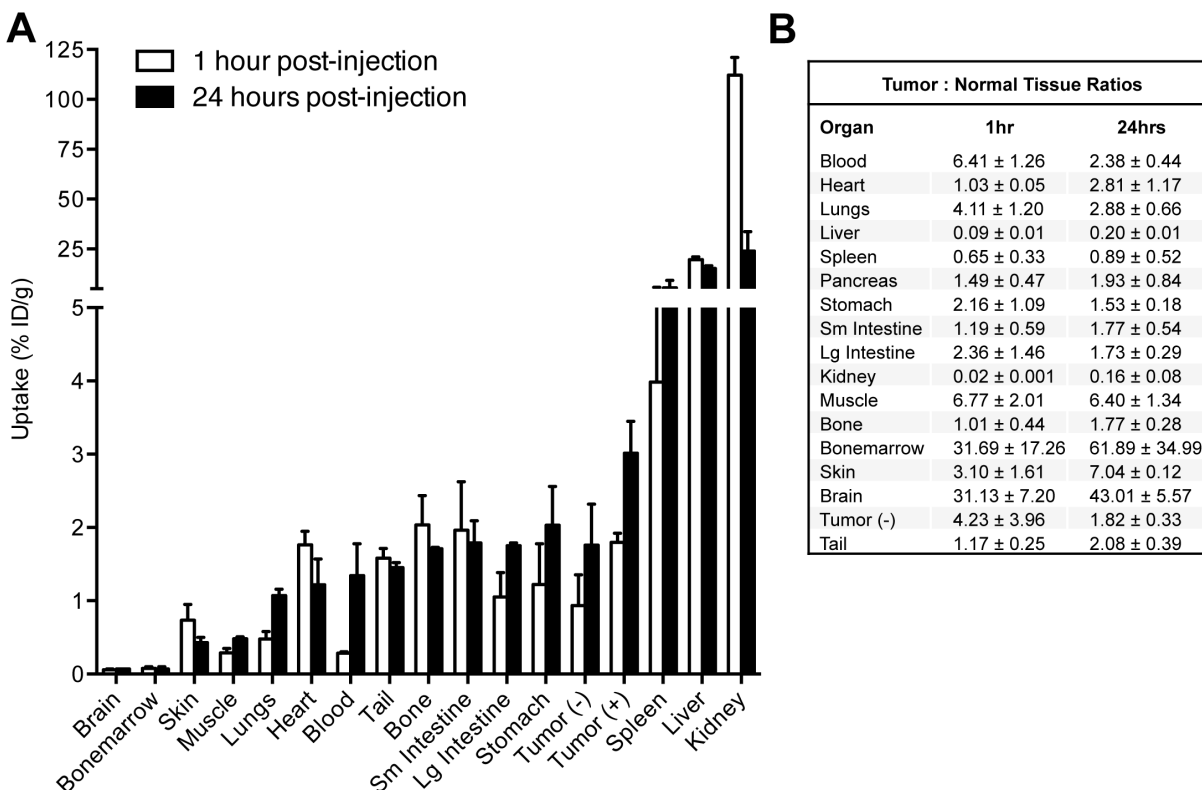**Figure S12**. 1 and 24 hour biodistribution of $^{64}$Cu-DOTA-HAC. (*A*) After completion of micro-PET/CT imaging, mice were euthanized and dissected for biodistribution analysis. Mean uptake in the indicated organs and tissues are given as the percentage of injected dose per gram of tissue (%ID/g). Error bars represent s.e.m. (*B*) Summary of means and s.e.m. of the ratios of tumor to tissue uptake at 1 and 24 hours.

| Primer | Sequence (5' to 3') |
|---|---|
| D1aff_1F | CATTTTCAATTAAGATGCAGTTACTTCGCTG |
| D1aff_2R | AATAACAGAAAATATTGAAAAACAGCGAAGTAACTGCATCTTAATTG |
| D1aff_3F | TTACTTCGCTGTTTTTCAATATTTTCTGTTATTGCTAGCGTTTTAGCAG |
| D1aff_4R | GTCTATCTGGGGAATCTGCTAAAACGCTAGCAATAACAGAAAAT |
| D1aff_5F | TTTTAGCAGATTCCCCAGATAGACCATGGAACCCACCAAC |
| D1aff_6R | CAACAAAGCTGGGGAGAAAGTTGGTGGGTTCCATGGTC |
| D1aff_7F | AACTTTCTCCCCAGCTTTGTTGGTCGTCACTGAAGGTGA |
| D1aff_8R | GAACAAGTGAAAGTAGCGTTATCACCTTCAGTGACGACCAA |
| D1aff_9F | GTGATAACGCTACTTTCACTTGTTCCTTCTCCAACACTTCC |
| D1aff_10R | GAAGGATTCGGAAGTGTTGGAGAAGGAACA |
| D1aff_11F | CAACACTTCCGAATCCTTCNDTTTGRWTTGGHWTAGAVWGTCCCCAVNTNDTVW WVYTNDTVNATTGGCTNHTTTCCCAGAAGATAGATCC |
| D1aff_12R | GAGTGACTCTGAATCTAGCATCTKGAHNTGGTNBGGATCTATCTTCTGGGAAA |
| D1aff_13F | AGATGCTAGATTCAGAGTCACTCAATTGCCAAAC |
| D1aff_14R | GGACATGTGGAAATCTCTACCGTTTGGCAATTGAGTGACTCTGA |
| D1aff_15F | CGGTAGAGATTTCCACATGTCCGTCGTCAGAGCTAGAAGAAACG |
| D1aff_16R | GTAAGTACCGGAATCGTTTCTTCTAGCTCTGACGAC |
| D1aff_17F | GAAACGATTCCGGTACTTACNWTTGTGGTGCTATTNCTNDTNHTSCTVNANYTCAA ATTAAGVRWTCCTTGAGAGCTGAATTGAG |
| D1aff_18R | GGATCCTCTTTCAGTGACTCTCAATTCAGCTCTCAAGGA |
| D1aff_19F | ATTGAGAGTCACTGAAAGAGGATCCGAACAAAGCTTATC |
| D1aff_20R | CAAGTCTTCTTCGGAGATAAGCTTTTGTTCGGATCCTCTT |
| D1aff_21F | AAAGCTTATCTCCGAAGAAGACTTGGGTGGTGGTGG |
| D1aff_22R | CCACCAGATCCACCACCACCCAAGTC |

**Table S1**. Primers used to create "First Generation" PD-1 library.

| Primer | Sequence (5' to 3') |
|---|---|
| 1F_AffMat_G2 | CATTTTCAATTAAGATGCAGTTACTTCGCTG |
| 2R_AffMat_G2 | AATAACAGAAAATATTGAAAAACAGCGAAGTAACTGCATCTTAATTG |
| 3F_AffMat_G2 | TTACTTCGCTGTTTTTCAATATTTTCTGTTATTGCTAGCGTTTTAGCAG |
| 4R_AffMat_G2 | GTCTATCTGGGGAATCTGCTAAAACGCTAGCAATAACAGAAAAT |
| 5F_AffMat_G2 | TTTTAGCAGATTCCCCAGATAGACCATGGAACCCACCAAC |
| 6R_AffMat_G2 | CAACAAAGCTGGGGAGAAAGTTGGTGGGTTCCATGGTC |
| 7F_AffMat_G2 | AACTTTCTCCCCAGCTTTGTTGGTCGTCACTGAAGGTGA |
| 8R_AffMat_G2 | GAACAAGTGAAAGTAGCGTTATCACCTTCAGTGACGACCAA |
| 9F_AffMat_G2 | GTGATAACGCTACTTTCACTTGTTCCTTCTCCAACACTTCC |
| 10R_AffMat_G2 | GAAGGATTCGGAAGTGTTGGAGAAGGAACA |
| 11F_AffMat_G2 | CCAACACTTCCGAATCCTTCVRTNTTNWTTGGYWTYDTSAWTCCCCATCCDRTCAAACTGATAMATTGGCTGCTTTCCCAGAAG |
| 12R_AffMat_G2 | GACCTGGTTGGGATCTATCTTCTGGGAAAGCAGCCAAT |
| 13F_AffMat_G2 | GAAGATAGATCCCAACCAGGTCMAGATGCTAGATTCAGARYTACTCAATTGCCAAACGGTAGAG |
| 14R_AffMat_G2 | CTTCTAGCTCTGACGACGGASANGTGGAAATCTCTACCGTTTGGCAATTGAG |
| 15F_AffMat_G2 | TCCGTCGTCAGAGCTAGAAGAAACGATTCCGGTACT |
| 16R_AffMat_G2 | GCTCTCAAGGATTCCTTAATTTGAANCTTTGGAGCAWRGGAAATARYACCACAAANAWRAGTACCGGAATCGTTTCTTCTAGC |
| 17F_AffMat_G2 | TTCAAATTAAGGAATCCTTGAGAGCTGAATTGAGAGTCAC |
| 18R_AffMat_G2 | GTTCGGATCCTCTTTCAGTGACTCTCAATTCAGCTCTCAAG |
| 19F_AffMat_G2 | GTCACTGAAAGAGGATCCGAACAAAGCTTATCTCCGAAGAAGAC |
| 20R_AffMat_G2 | CCACCAGATCCACCACCACCCAAGTCTTCTTCGGAGATAAGCTTTTG |

**Table S2**. Primers used to create "Second Generation" PD-1 library.

| Day 14 comparison | Mean Diff. | 95% CI of diff. | Significant? | Summary | Individual P value |
|---|---|---|---|---|---|
| PBS vs. HACmb | 507.6 | 320.1 to 695.2 | Yes | **** | < 0.0001 |
| PBS vs. anti-PD-L1 | 69.97 | -117.6 to 257.5 | No | ns | 0.4636 |
| PBS vs. anti-CTLA4 | 480.7 | 293.2 to 668.3 | Yes | **** | < 0.0001 |
| PBS vs. anti-CTLA4+HACmb | 747.4 | 559.9 to 935.0 | Yes | **** | < 0.0001 |
| PBS vs. anti-CTLA4+ anti-PD-L1 | 510.4 | 322.8 to 697.9 | Yes | **** | < 0.0001 |
| HACmb vs. anti-PD-L1 | -437.7 | -625.2 to -250.1 | Yes | **** | < 0.0001 |
| HACmb vs. anti-CTLA4 | -26.92 | -214.5 to 160.6 | No | ns | 0.7779 |
| HACmb vs. anti-CTLA4+HACmb | 239.8 | 52.21 to 427.3 | Yes | * | 0.0124 |
| HACmb vs. anti-CTLA4+ anti-PD-L1 | 2.740 | -184.8 to 190.3 | No | ns | 0.9771 |
| anti-PD-L1 vs. anti-CTLA4 | 410.8 | 223.2 to 598.3 | Yes | **** | < 0.0001 |
| anti-PD-L1 vs. anti-CTLA4+HACmb | 677.4 | 489.9 to 865.0 | Yes | **** | < 0.0001 |
| anti-PD-L1 vs. anti-CTLA4+ anti-PD-L1 | 440.4 | 252.9 to 628.0 | Yes | **** | < 0.0001 |
| anti-CTLA4 vs. anti-CTLA4+HACmb | 266.7 | 79.13 to 454.2 | Yes | ** | 0.0055 |
| anti-CTLA4 vs. anti-CTLA4+ anti-PD-L1 | 29.66 | -157.9 to 217.2 | No | ns | 0.7559 |
| anti-CTLA4+HACmb vs. anti-CTLA4+ anti-PD-L1 | -237.0 | -424.6 to -49.47 | Yes | * | 0.0134 |

**Table S3.** Statistical analysis of large tumor study groups at treatment day 14.